HEAT TRANSFER ENHANCEMENT WITH TUBE INSERTS
How Can We Define the Best Benefit?

by

Ventsislav D. ZIMPAROV**, *Plamen J. PENCHEV*, *and Plamen J. BONEV

Department of Mechanical Engineering, Gabrovo Technical University, Gabrovo, Bulgaria

Original scientific paper
https://doi.org/10.2298/TSCI240702225Z

This study recommends the use of two criteria FG-1a and FG-1b for evaluating the benefits that could be obtained when different heat transfer enhancement techniques are implemented in the heat exchanger design, instead of the most commonly used criterion PEC, based on the constraint of fixed pumping power. When the thermal performances of two heat transfer channels are compared, they must be put under equal conditions, such as fixed heat transfer area, mass-flow, and initial temperature. It is also important whether an external thermal resistance of the channel is available or not. The first case is typical for experiments in shell-and-tubes heat exchangers where the objective is an increase in the heat flow, whereas the second case is encountered in experiments with electrical heating of the tube wall, where the objective is a decrease in the driving temperature difference with fixed heat flow. An additional constraint in both cases is the augmentation entropy generation number, $N_{sa} \leq 1$. Through manifold examples, using different twisted tape inserts, we demonstrate how these two criteria have to be implemented for assessing the thermal benefits. The use of the criterion PEC is connected with many erroneous results and misunderstood conclusions that have been revealed in this study.

Key words: *twisted tape inserts, criteria for assessment, entropy generation number, performance benefits*

Introduction

The tube inserts as heat transfer enhancement techniques have been known for many years since they are easy to install and operate [1-5]. Despite they have been recognized and used for more than a century, the efforts to improve their thermal performance by modifying their design differently are continuing [6-10].

The implementation of the tube inserts can be classified into several common groups: single tube inserts with different modifications (simple augmentation technique) [11-18]. A combination of several tube inserts in the channel (compound heat transfer augmentation technique) [19-23], and a combination of tube inserts with nanofluid as a working media [24-26].

*Corresponding author, e-mails: ventsi.zimparov@gmail.com; vdzim@tugab.bg

Criteria for performance evaluation

When an augmentation heat transfer technique is applied to improve the thermal performance of a heat exchanger, the selection of an appropriate criterion for evaluation of the benefit depends on the objective that has been imposed and the way for gathering the experimental data for the heat transfer coefficient. The most common way to select the experimental data is to use an experimental set-up as a double-pipe counterflow heat exchanger or channel with electrical heating. The augmentation heat transfer technique in the channel could be *surface roughness* on the tube wall, inserts in the internal flow, or a combination of both of them. When a double-pipe counterflow heat exchanger is used, an outside-of-the-wall thermal resistance exists and it has to be taken into consideration. In the case of electrical heating of the wall, the outside thermal resistance does not exist and the objective that has to be pursued is different.

Bergles *et al*. [27] proposed first many performance evaluation criteria according to the objective pursued and the constraints imposed. One of these criteria, R_3, named later performance evaluation criteria (PEC), is still used immensely [14-26]. The objective of this criterion is increased heat duty with a major constraint of fixed pumping power:

$$PEC \equiv R_3 = \frac{\mathrm{Nu_a}/\mathrm{Nu_s}}{\left(f_a/f_s\right)^{1/3}} \tag{1}$$

Durán-Plazas *et al.* [28] and Picon-Nunez *et al.* [29] introduced a mapping plot to select the best promoter geometries using thermal and pressure drop irreversibility analysis. This performance evaluation criterion is a modification of PEC, eq. (1), with the same constraint of fixed pumping power. The disadvantages of the criterion PEC have been discovered in [30], whereas the development of the criteria of Bergles *et al.* [27] was made by Webb [31].

Bejan [32] was the pioneer who introduced a parameter evaluating the rate of entropy generation, named *augmentation entropy generation number*, N_{sa}, and defined as:

$$N_{sa} = \frac{1}{1+\phi_s}\left(N_T + \phi_s N_P\right) \tag{2}$$

where N_T and N_P are the values of N_{sa} in the limits $\phi_s \to 0$ and $\phi_s \to \infty$. The requirement for thermodynamic efficiency is the fulfillment of the condition $N_{sa} < 1$. Heat transfer enhancement technique giving $N_{sa} > 1$ is inefficient and must be dismissed. Zimparov *et al*. [33] have suggested that the imposed constraint for fixed pumping power must be removed from the list of constraints and replaced with the constraint $N_{sa} \le 1$. It has to be noted that, when two channels are compared, the requirement for thermodynamic efficiency $N_{sa} < 1$ has been imposed by Bejan [32] under the constraints of fixed heat and mass-flows $Q_* = 1$, $W_* = 1$ and fixed geometry $A_* = 1$. Then, the criteria of Webb [31] could been substantially reduced to three [33]. Two of them, namely: FG-1a, FG-1b will be applied for evaluation of the benefits in the *retrofit* applications, as:

FG-1a (fixed geometry criterion) – objective $Q_* > 1$ and
FG-1b (fixed geometry criterion) – objective $\Delta T_i^* < 1$.

The criterion FG-1a is applied in the case when different tube inserts are used in the shell-and-tube heat exchanger to increase their heat duty, whereas the criterion FG-2a has to be used in the case of solar air heaters or solar water collectors to evaluate the decrease in the driving temperature difference. In the second case, the heat flux falling on the absorber surface is constant, equal for the two comparable channels and the reduction of the driving temperature difference by the reduction of the wall temperature of the channel is the benefit. The reduction of the wall temperature decreases the heat losses to the surroundings and increases the thermal efficiency of the solar collector.

Objectives

This paper is a continuation of the ideas developed in [33] and by many examples demonstrates why the two criteria, FG-1a, and FG-1b [33] must be used, instead of the criterion PEC, eq. (1), for evaluating the benefits that can be obtained by the implementation of different heat transfer enhancement techniques in the case of *retrofit*. We demonstrate this by the use of the experimental results of Dagdevir and Ozceyhan [14] and Heeraman *et al.* [15]. The criterion FG-1a will be applied using the experimental data of Heeraman *et al.* [15] obtained by experiments in a double pipe counter flow heat exchanger, whereas the criterion FG-1b will be used with the experimental data of Dagdevir and Ozceyhan [14] obtained through experiments with electrical heating of the tube wall.

Benefit equations

The benefit equations are discussed and documented in detail in [30, 31, 33]. The fixed geometry criteria cases involve a replacement of smooth tubes by augmented tubes of equal diameter and length and may be regarded as *retrofit* applications. Two cases can be encountered: FG-1a and FG-1b.

Case FG-1a

The objective of the case FG-1a is an increase in the heat flow, $Q_* > 1$with the constraints $W_* = 1$, $A_* = 1$ (with $D_* = 1$, $N_* = 1$, and $L_* = 1$), $\Delta T_\mathrm{i}^* = 1$, and additional constraint $N_\mathrm{sa} \le 1$ [33]. The pumping power will increase, $P_* = f_* > 1$and if the installed pumping power is not enough to meet the increase in hydraulic friction, it should be changed with another one [31]. The formulation of a PEC requires relations that define the heat transfer and friction characteristics relative to the reference exchanger [31] and take into account the thermal resistance across the metal tube wall, a tube side fouling resistance, and a possibility of enhancement simultaneously on the inner and outer tube surfaces for a two-fluid heat exchanger.

The *UA* equations for the reference (smooth tube) and augmented exchangers are:

$$\frac{1}{U_\mathrm{s} A_\mathrm{s}} = \frac{1}{h_\mathrm{s} A_\mathrm{s}} + \frac{1}{h_\mathrm{os} A_\mathrm{os}} + \frac{\delta}{k_\mathrm{w} A_\mathrm{m}} + \frac{R_\mathrm{f}}{A_\mathrm{s}} \tag{3a}$$

$$\frac{1}{UA} = \frac{1}{h_\mathrm{a} A_\mathrm{a}} + \frac{1}{h_\mathrm{o} A_\mathrm{o}} + \frac{\delta}{k_\mathrm{w} A_\mathrm{m}} + \frac{R_\mathrm{f}}{A} \tag{3b}$$

Following Webb [31], with the constraints imposed, the relative overall heat conductance equation is:

$$(UA)_* = \frac{1+\beta_\mathrm{s}}{\mathrm{Nu}_*^{-1} + \beta} \tag{4}$$

with β_s and β as thermal composite resistances defined by Webb [31] (see tab. 2, p. 719 [35]). The augmented and smooth exchangers may not operate at the same effectiveness, ε. For these cases the ε-NTU method [31], gives:

$$Q_* = W_* \varepsilon_* \Delta T_i^* \tag{5}$$

where ΔT_i is the temperature difference between the two inlet streams. For fixed ratios of the inlet temperatures, ΔT_i^*, and mass-flow rates $W_* = 1$, eq. (5) yields:

$$Q_* = \varepsilon_* \tag{6}$$

Since the operating conditions of the smooth tube exchanger are known, number of thermal units $NTU_s = U_s A_s / W_s C_p$ is known and ε_s is calculable. Once $(UA)_*$ for the augmented exchanger is known, and the $(NTU)_a$ is calculated by:

$$NTU_a = NTU_s (UA)_* \tag{7}$$

Then ε_a of the augmented exchanger may be calculated and Q_* can be obtained from eq. (6). The constraint $N_{sa} \le 1$, eq. (2) yields:

$$N_{sa} = \frac{1}{1+\phi_s}\left\{\frac{Q_*^2}{\mathrm{Nu}_*} + \phi_s f_*\right\} \tag{8}$$

where the ratio, ϕ_s, is to be calculated following Bejan [32] (Chapter 6, p. 120).

Case FG-1b

This case pursues a decrease in the inlet temperature difference $\Delta T_i^* < 1$ and the driving temperature difference $\Delta T_m^* < 1$, with the constraints $Q_* = 1$, $W_* = 1$, $A_* = 1$, and $N_{sa} \le 1$ [33]. When $Q_* = 1$ and $W_* = 1$, Eq. (5) yields:

$$\Delta T_i^* = \varepsilon_*^{-1} \tag{9}$$

Whereas N_{sa} becomes:

$$N_{sa} = \frac{1}{1+\phi_s}\left(\frac{1}{\mathrm{Nu}_*} + \phi_s f_*\right) \tag{10}$$

Results and discussion

In this part, we show how the real benefit is obtained, by the use of some twisted tape inserts as a heat transfer augmentation technique for single-phase fluid flow in tubes, if the constraint $N_{sa} \le 1$ is imposed, instead of the fixed pumping power. The experimental data for Nu_a *vs*. Reynolds number and f_a *vs*. Reynolds number of Heeraman *et al.* [15] and Dagdevir and Ozceyhan [14] will be used for this manifestation.

First of all, however, it has to be understood why the two kinds of enhanced surfaces, with or without outside thermal resistance of the surface under consideration, have to be evaluated through the different criteria, FG-1a or FG-1b. When Bejan [32] invented the criterion for thermodynamic efficiency, $N_{sa} < 1$, two channels were compared and subjected to the constraints as: $A_* = 1$, $L_* = 1$, $W_* = 1$, and $Q_* = 1$. This corresponds to the case FG-1b [33], with objective $\Delta T_i^* < 1$, constraint $N_{sa} < 1$, and when the outside thermal resistance is not available (experimental studies with electrical heating of the tube wall are related to this case).

Case FG-1a

When the experimental data for heat transfer coefficient and friction factor are collected in a two-fluid heat exchanger, the existence of the outside fluid thermal resistance impacts the increase in the heat flow $Q_* > 1$ and has to be taken into consideration. To demonstrate how the criterion FG-1a applies to assessing the benefit, the experimental data from the study of Heeraman *et al.* [15] will be used. In this study, water was used as a working fluid in a double-pipe heat exchanger. The twisted tape inserts having different dimple and hole configurations occupied the inner tube. The geometrical characteristics of the twisted tapes were a twist ratio of 5.5 and a dimple diameter-to-depth ratio D/H of 1.5, 3.0, and 4.5.

Based on the thermal and hydraulic characteristics for Nu_a *vs*. Reynolds number and f_a *vs*. Reynolds number published in [15], the variation of the heat flow ratio Q_* with Reynolds number has been calculated and depicted in fig. 1(a). It must be noted, that the values of Q_*, presented in fig. 1(a), have been obtained by the lack of an outside thermal resistance. That means that the increase in Q_* is the maximum benefit that can be achieved. However, the penalty is an increase in the entropy generation, $N_{sa} > 1$, fig. 1(b). That means, that the constraint $N_{sa} \leq 1$ has not been fulfilled.

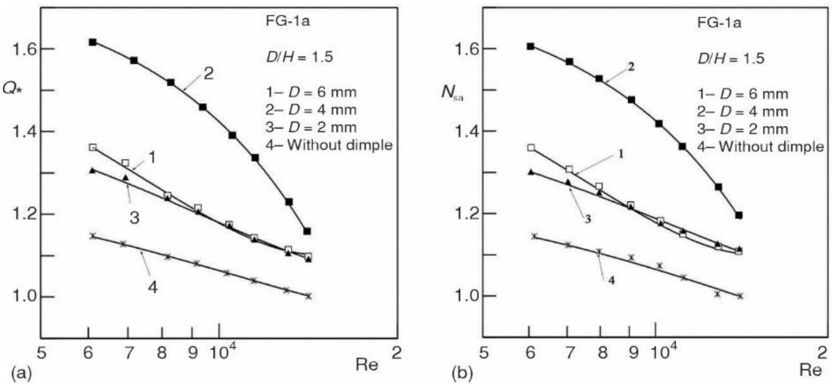

Figure 1. (a) Variation of the ratio Q_* with Reynolds number and (b) variation of the augmentation entropy generation number N_{sa} with Reynolds number (data from [15]);
Remark: For all figs. 1 to 10, the abscissa labels must be read as: for Re < 10^4, 5,6,..9 mean $5\cdot10^3$ etc., whereas for Re > 10^4, 2 means $2\cdot10^4$)

Since, there is no information related to this thermal resistance in [15], an outside thermal resistance $1/h_oA_o = 0.011$ K/W from our experimental program [34], responding to the range Re = (6-14)$\cdot10^3$ [15], has been included in the calculations of Q_*. Figure 2(a) presents the variations of the real benefit, $Q_* > 1$ whereas fig. 2(b) shows how the new N_{sa} varies with Reynolds number. As seen, the twisted tape without dimple (tape 4) does not give any benefit, $Q_* < 1$ and it should be excluded from the consideration. Among the other three tapes, tape 2 (D = 6 mm) can bring about the greatest benefit 5%-13%, but this benefit gradually decreases with the increase in Reynolds number. The results of the augmentation entropy generation number N_{sa}, fig. 2(b), reveal that the requirement $N_{sa} \leq 1$ is fulfilled for the rest of twisted tapes 1-3. The best characteristic of N_{sa} with Reynolds number (the smallest value of N_{sa}) is again tape 2.

The other experimental data of Heeraman *et al.* [15] for D/H = 3.0 and D/H = 4.5 can be presented similarly. As seen from fig. 3, D/H = 3.0, the variations of the Q_* with Reynolds number and N_{sa} with Reynolds number have a similar behavior as those of fig. 2. In this case, the greatest benefit can be obtained by the twisted tape 6. However, the variation of Q_* with Reynolds number for D/H = 4.5, fig. 4, is completely different: all twisted tape geometrical configurations possess $Q_* < 1$and are defined as inefficient and without any benefit. That is why, they will not be considered anymore.

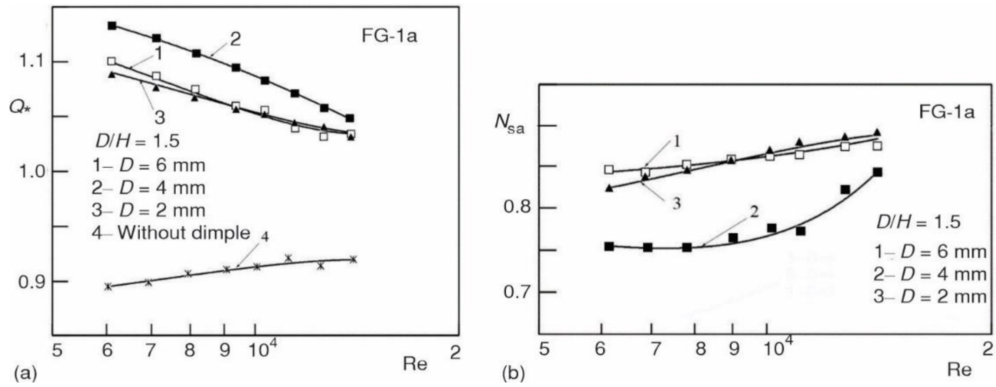

Figure 2. (a) Variation of Q_* with Reynolds number and (b) variation of N_{sa} with Reynolds number (data from [15])

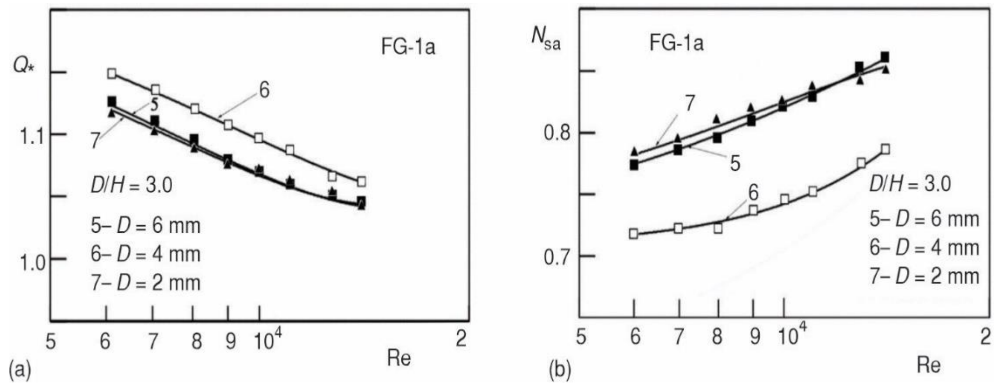

Figure 3. (a) Variation of $Q_*$with Reynolds number and (b) variation of N_{sa} with Reynolds number (data from [15])

To define the best-twisted tape geometrical configuration from all, it is needed to use a general criterion in the form:

$$N_s^+ = \frac{N_{sa}}{Q_*} \tag{11}$$

that pursues two objectives simultaneously: minimum augmentation entropy generation number $N_{sa} < 1$ and maximum benefit $Q_* > 1$.

The results from the use of this criterion, eq. (11), are shown in fig. 5 for the cases $D/H = 1.5$ and $D/H = 3.0$, whereas the best configurations 2 and 6 are presented in fig. 6. As seen, the best-twisted tape geometrical configuration from the all is number 6, which will bring about the greatest benefit $Q_* > 1$, together with the minimum $N_{sa} < 1$. It has to be noted, however, that this benefit is only 15%, for the smallest Reynolds number studied, and gradually decreases with the increase in Reynolds number, fig. 3(a).

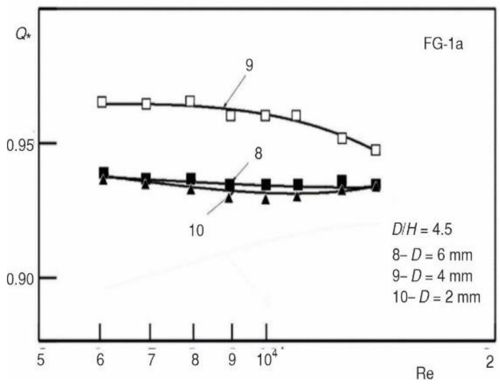

Figure 4. The variation of the ratio $Q_*$with Reynolds number (data from [15])

The use of the criterion PEC, eq. (1), by Heeraman *et al.* [15] for evaluation of the benefits of the twisted tape geometrical configurations studied, revealed that all of them, except for the case $D = 4$ mm, $D/H = 3$, and $\mathrm{Re} < 8\cdot10^3$ experienced PEC < 1 (see fig. 11, [17]), *i.e.*, no benefits were available. That means, that the use of the criterion PEC, eq. (1), leads to erroneous results concerning the assessment of existing benefit and its merit. These results are due to the constraints imposed as:

- the same driving temperature difference,
- two heat exchangers work at different Reynolds number due to the fixed pumping power, and
- the lack of the outside heat transfer thermal resistance is unacceptable for the shell-and-tube heat exchangers, where the "retrofit" operation is applied (for more details see [30, 33].

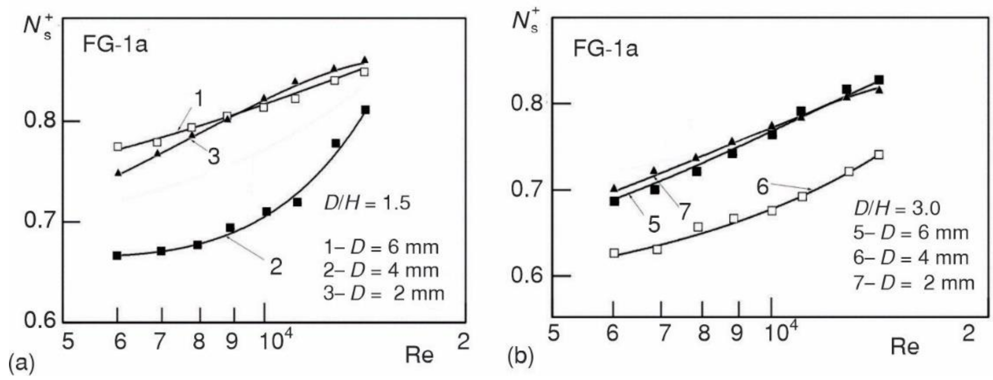

Figure 5. The variation of the general criterion N_S^+ with Reynolds number; (a) *D*/*H* = 1.5 and (b) *D*/*H* = 3.0

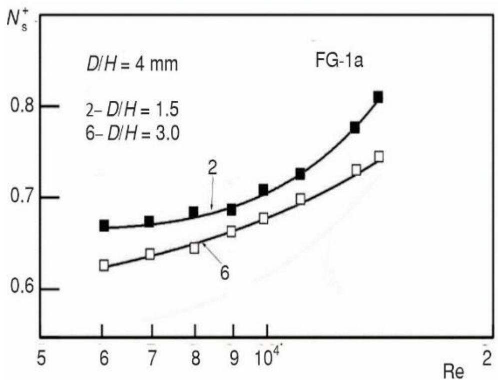

Figure 6. The variation of the general criterion N_S^+ with Reynolds number (*D*/*H* = 1.5; 3.0)

Case FG-1b

As mentioned foregoing, the criterion FG-1b is used in the cases when the thermal resistance outside of the tube wall does not exist. All experiments with electrical heating of the tube wall are subjected to this criterion. In this section, we demonstrate how the criterion FG-1b applies to assessing the benefit using the study of Dagdevir and Ozceyhan [14]. They investigated the thermal and hydraulic characteristics of different twisted tapes with geometrical parameters such as twist ratio $p_p/y = 5.88$ and dimpled pitch ratio $p_d/y = 0.25$, 0.5, 1.0. Water and mixtures of water and ethylene glycol were used as a working fluid in the range $\mathrm{Re} = (5.2 - 22.8)\cdot10^3$. The tube wall was heated by constant heat flux. On the base of the experimental data, the variations of ΔT_i^* and N_{sa} have been calculated using eqs. (9) and (10), and presented in figs. 7-9.

The variations of ΔT_i^* and N_{sa} with Reynolds number (experiments with water, $\mathrm{Pr} = 6.0$) are presented in fig. 7. The variations of ΔT_i^* and N_{sa} with Reynolds number are very close, since $\phi_s \ll 1$. Besides, ΔT_i^* and N_{sa} are connected and have the same behavior. As seen in fig. 7(b), all twisted tape configurations reduce the entropy generation, $N_{sa} < 1$, but the greatest benefit $\Delta T_i^* < 1$ can be obtained by configuration 3 ($p_d/y = 0.25$), fig. 7(a). The behavior of configuration 5 ($p_d/y = 0.50$), fig. 7(b), is also interesting. The curve N_{sa} vs. Reynolds number has a minimum at Re ≈ $1.8 \cdot 10^4$ where the benefits of configurations 3 and 5 equalize.

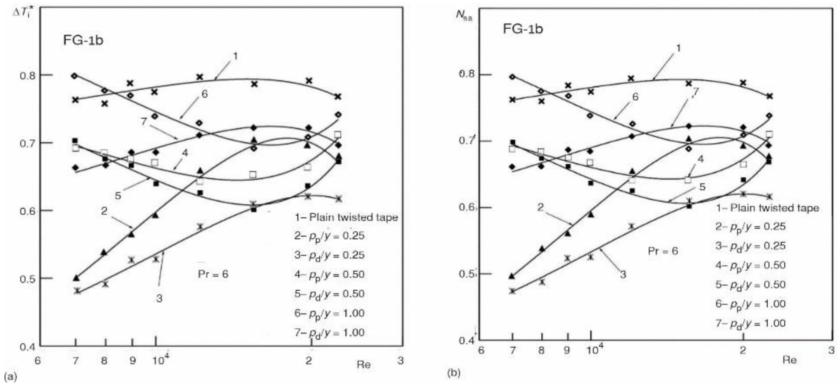

Figure 7. (a) Variation of ΔT_i^* with Reynolds number and (b) variation of N_{sa} with Reynolds number Pr = 6.0 (data from [14])

It should also be noted that the benefit from the use of configurations 1, 2, 3, and 7 increases with the decrease in Reynolds number, whereas configurations 4, 5, and 6 are experienced on the opposite.

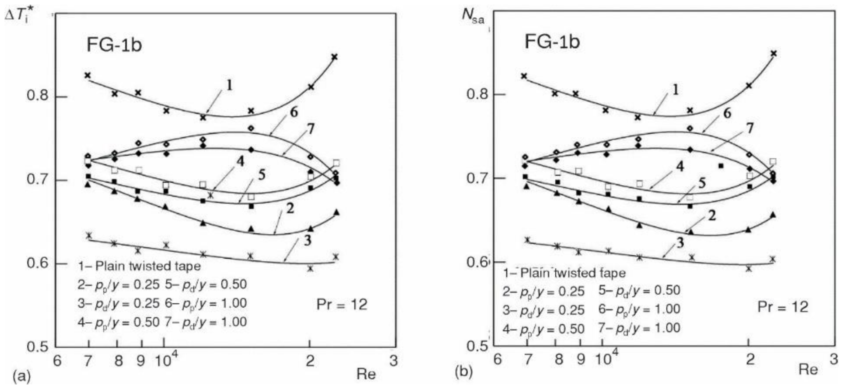

Figure 8. (a) Variation of ΔT_i^* with Reynolds number and (b) variation of N_{sa} with Reynolds number Pr = 12.0 (data from [14])

Figure 8 presents the variations of ΔT_i^* and N_{sa} with Reynolds number, for Pr = 12.0. As seen, the twisted tape configuration 3 ($p_d/y = 0.25$) possesses the best performance, giving the greatest benefit. Another feature of the most of the curves (1,2,3,4,5) is that they have experienced minimum values for ΔT_i^* and N_{sa}.

The variations of ΔT_i^* and N_{sa} with Reynolds number, for Pr = 20, are depicted in fig. 9. For this value of Prandtl number, two regions of Reynolds number can be specified, where a particular twisted tape configuration assures the greatest benefit of $\Delta T_i^* < 1$ and $N_{sa} < 1$: in the region Re < $9 \cdot 10^3$, the twisted tape configuration 2, $p_d/y = 0.25$, is to be preferred, whereas for Re < $9 \cdot 10^3$, the twisted tape configuration 3, $p_d/y = 0.25$, brings about the greatest benefit.

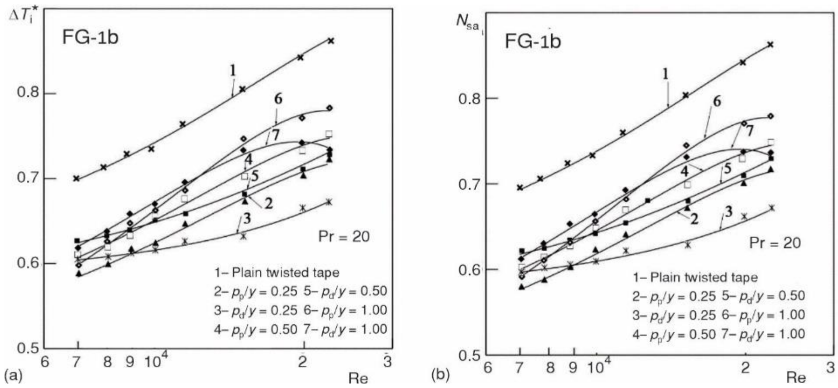

Figure 9. (a) Variation of ΔT_i^* with Reynolds number and (b) variation of N_{sa} with Reynolds number, Pr = 20 (data from [14])

The results in figs. 7-9 reveal that among all studied twisted tape configurations, the most attractive and with the highest thermal performance coefficient is the twisted tape configuration 3 (p_d/y = 0.25), which depends on Reynolds number and Prandtl number. Figure 10 shows how the benefit of tape configuration 3 (p_d/y = 0.25), $\Delta T_i^* < 1$, varies according to the values of Reynolds number and Prandtl number. As seen, when Re < $1.6 \cdot 10^4$, water is the most appropriate and beneficial fluid for the goal, whereas, in the range Re > $1.6 \cdot 10^4$, the ethylene and water mixture (20:80) (with Pr = 12) is the best choice.

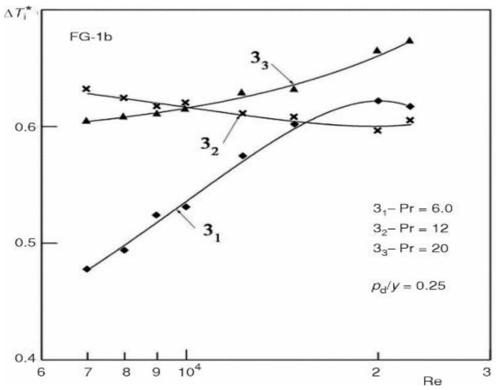

Figure 10. The variation of ΔT_i^* with Reynolds number – comparison between the greatest benefits

To assess the benefits of the different twisted tape inserts studied, Dagdevir and Ozceyhan [14] used the criterion PEC, eq. (1), developed with the constraint of fixed pumping power. This criterion is close to the criterion FG-2a [31], but not the same. The calculated PEC results for water-ethylene glycol mixtures are presented in fig. 15 (see in [14]), where can be seen that when the ethylene glycol in the mixture increases (Prandtl number increases), the benefit gradually decreases and for Pr = 20 completely disappears.

Conclusions

This study recommends the use of two criteria FG-1a and FG-1b for evaluating the benefits that could be obtained when different heat transfer enhancement techniques are implemented in the heat exchanger design, instead of the most commonly used criterion PEC, based on the constraint of fixed pumping power. When the thermal performances of two heat transfer channels are compared, they must be put under equal conditions, such as fixed heat transfer area, mass-flow, and initial temperature of the flow. It is also important whether an external thermal resistance of the channel is available or not. The first case is typical for experiments in shell-and-tubes heat exchangers where the objective is an increase in the heat flow, whereas the second case is encountered in experiments with electrical heating of the tube wall, where the objective is a decrease in the driving temperature difference with fixed heat flow. An additional constraint in both cases is the augmentation entropy generation number $N_{sa} \leq 1$.

Through manifold examples, using different twisted tape inserts in the studies of Heeraman *et al.* [15] and Dagdevir and Ozceyhan [14], we demonstrate how these two criteria have to be implemented for assessing the thermal benefits. The use of the criterion PEC, eq. (1), is connected with many erroneous results and misunderstood conclusions that have been revealed in this study. When augmentation heat transfer techniques are implemented in two-fluid heat exchangers or one-fluid heat exchangers, they pursue completely different objectives: in a two-fluid heat exchanger the objective is $Q_* > 1$, whereas in a one-fluid heat exchanger, the objective is the decrease in the tube wall temperature and the driving temperature difference through $\Delta T_i^* < 1$. The constraint $N_{sa} < 1$ is compulsory and critical to be obeyed in both cases.

The global optimization strategy of minimizing entropy generation pertains to the most efficient use of energy in heat transfer equipment. We must emphasize in this context that there are clear economic benefits involved. This will specifically lead to minimal energy usage and appropriate equipment design, regardless of the energy cost, which is highly reliant on local energy production and accessible sources. This study does not cover an economic analysis related to economic evaluation. It varies greatly depending on the manufacturer and is dependent upon the design and construction of the heat transfer equipment. When it comes to *retrofit*, the cost of implementing various twisted tape inserts can be occasionally low.

Acknowledgment

This study has been supported by the Project 2201 M/2024 of the Technical University of Gabrovo, Bulgaria.

Nomenclature

A	– heat transfer surface area, [m^2]
A_*	– ratio of heat transfer surfaces, (= A_a/A_s)
D	– tube diameter or dimple diameter, [m]
D_*	– ratio of tube diameters, (= D_a/D_s), [–]
f	– Fanning friction factor, [–]
f_*	– ratio of Fanning friction factors (= f_a/f_s), [–]
G	– mass velocity, [kgs^{-1}m^{-2}]
G_*	– ratio of mass velocities, (= G_a/G_s), [–]
h	– heat transfer coefficient, [Wm^{-2}K^{-1}]
H	– half of the twisted tape pitch, [m]
L	– tube length [m]
L_*	– ratio of tube lengths, (= L_a/L_s)
N_*	– ratio of number of tubes, (= $N_{t,a}/N_{t,s}$), [–]
Nu	– Nusselt number, [–]
Nu$_*$	– ratio of Nusselt numbers, (= Nu$_a$/Nu$_s$), [–]
N_{sa}	– augmentation entropy generation number, [–]
p	– pumping powers, [W]
P_*	– ratio of pumping powers, (= p_a/p_s), [–]
Pr	– Prandtl number, [–]
Q	– heat transfer rates
Q_*	– ratio of heat transfer rates, (= Q_a/Q_s), [–]
Re	– Reynolds number, [–]
R_f	– fouling thermal resistance, [W^{-1}m^{2}K]
ΔT	– temperature difference, [K]
ΔT_i^*	– ratio of inlet temperature difference between hot and cold streams, (=$\Delta T_{i,a}/\Delta T_{i,s}$), [–]
U	– overall heat transfer coefficient, [Wm^{-2}K^{-1}]
y	– twist pitch length, [m]
W	– mass-flow rate in heat exchanger, [kgs^{-1}]
W_*	– ratio of mass-flow rates, (= W_a/W_s), [–]

Greek symbols

β	– composite thermal resistance, [W^{-1}m^{2}K]
ε_*	– ratio of heat exchanger effectiveness, (= $\varepsilon_a/\varepsilon_s$), [–]
ϕ_s	– irreversibility distribution ratio, [–]

Subscripts

a	– augmentation
d	– dimpled
i	– inlet
m	– mean

o – outlet or outside
p – perforated
s – smooth

References

[1] Whitham, J. M., The Effect of Retarders in Fire Tube Boilers, *Street Journal*, *12* (1896), 6, 374

[2] Manglik, R. M., Bergles, A. E., Swirl Flow Heat Transfer and Pressure Drop with Twisted Tape Inserts, in: *Advances in Heat Transfer* (eds. J.P. Hartnett, *et al*.) Academic, New York, USA, 2002, vol. 36, pp. 183-266

[3] Manglik, R. M., Heat Transfer Enhancement, in: *Heat Transfer Handbook* (eds. A. Bejan and A.D. Kraus), Wiley, New York, USA, 2003, pp. 1029-1130

[4] Webb, R. L., Kim, N. H., *Principal of Enhanced Heat Transfer*, Taylor and Francis Group, New York, USA, 2005, pp. 207-243.

[5] Saha, S. K., *et al.*, *Introduction of Enhanced Heat Transfer*, Springer, New York, USA, 2020, pp. 17-72

[6] Zimparov, V., *et al*., Performance Evaluation of Tube-in-Tube Heat Exchangers with Heat Transfer Enhancement in the Annulus, *Thermal Science, 10* (2006), 1, pp. 45-56

[7] Zimparov, V., *et al*., Benefits from the Use of Wire-Coil Inserts in Water Transitional and Low Turbulent Flow – The Influence of the Wire-Coil Pitch, *Thermal Science*, 26 (2022), 4B, pp. 3597-3604

[8] Bucak, H., Yielmaz, F., The Current State on the Thermal Performance of Twisted Tapes: A Geometrical Categorization Approach, *Chemical Engineering & Processing: Process Intensification, 153* (2020), 107929

[9] Mousa, M. H., *et al.*, Review of Heat Transfer Enhancement Techniques for Single Phase Flows, *Renewable Sustainable Energy Reviews, 137* (2021), 110566

[10] Duran-Plazas, P., *et at*., Selection of Tube Inserts in Heat Exchanger Retrofit Applications for Increased Energy Recovery, *Cleaner Energy Systems, 3* (2022), 100024

[11] Selvam, S., *et al*., Experimental Studies on Effect of Bonding the Twisted Tapes with Pins to the Inner Surface of the Circular Tube, *Thermal Science*, *18* (2014), 4, pp. 1273-1283

[12] Maradiya, C., *et al.,* The Heat Transfer Enhancement Techniques and Their Thermal Performance Factor, *Beni-Suef University Journal of Basic and Applied Sciences, 7* (2018), 1, pp. 1-21.

[13] Abdulhamed, A.J., *et al.,* Tubular Heat Enhancement Using Twisted Tape Inserts with Large Holes, *Energy Engineering, 121* (2024), 2, pp. 273-280

[14] Dagdevir, T., Ozceyhan, V., An Experimental Study on Heat Transfer Enhancement and Flow Characteristics of a Tube with Plain, Perforated and Dimpled Twisted Tape Inserts, *International Journal of Thermal Science*, *159* (2021), 106564

[15] Heeraman, J., *et al.*, Experimental Evaluation and Thermal Performance Analysis of a Twisted Tape with Dimple Configuration in a Heat Exchanger, *Case Studies in Thermal Engineering, 46* (2023), 103003

[16] Karagoz, S., *et al.*, Experimental Investigation of the Effect of Wave Turbulators on Heat Transfer in Pipes, *Thermal Science*, *26* (2022), 2C, pp. 1771-1783

[17] Vishwakarma, D. K., *et al.,* Evaluating the Heat Transfer and Pressure Drop in the Transitional Flow Regime for a Horizontal Circular Tube Fitted with Wavy-Tape Inserts, *International Journal of Thermal Science, 196* (2024), 108677

[18] Vashistha, C., *et al.,* Experimental Investigation of Heat Transfer and Pressure Drop in a Circular Tube with Multiple Inserts, *Applied Thermal Engineering, 96* (2016), Mar., pp. 117-129

[19] Eiamsa-ard, S., *et al.,* Thermal Performance Evaluation of Heat Exchanger Tubes Equipped with Coupling Twisted Tapes, *Experimental Heat Transfer, 26* (2013), 5, pp. 413-430

[20] Bhattacharyya, S., *et al.,* Turbulent Flow Heat Transfer Through a Circular Tube with Novel Hybrid Grooved Tape Inserts: Thermohydraulic Analysis and Prediction by Applying Machine Learning Model, *Sustainability, 13* (2021), 6, 3068

[21] Bhuiya, M. M. K., *et al.*, Performance Assessment in a Heat Exchanger Tube Fitted with Double Counter Twisted Tape Inserts, *International Communications in Heat and Mass Transfer, 50,* (2014), Jan., pp. 25-33

[22] Bhuiya, M. M. K., *et al.*, Thermal Characteristics in a Heat Exchanger Tube Fitted with Triple Twisted Tape Inserts, *International Communications in Heat and Mass Transfer, 48* (2013), Nov., pp. 124-132

[23] Tamna, S., *et al.*, Heat Transfer Enhancement in Tubular Heat Exchangers with Double V-Ribbed Twisted-Tapes, *Case Studies in Thermal Engineering, 7* (2016), Mar., pp. 14-24

[24] Singh, S. K., Sarkar, J., Improving Hydrothermal Performance of Double-Tube Heat Exchanger with Modified Twisted Tape Inserts Using Hybrid Nanofluid, *Journal of Thermal Analysis and Calorimetry, 143* (2021), Feb., pp. 4287-4298
[25] Mozaffari, J., *et al.*, Experimental Investigation of Enhancing Influence of Al_2O_3 Nanoparticles on the Convective Heat Transfer in a Tube Equipped with Twisted Tape Inserts, *Thermal Science, 25*, (2021), 1B, pp. 541-551
[26] Singh, S. K., Sarkar, J., Experimental Hydrothermal Characteristics of Concentric Tube Heat Exchanger with V-Cut Twisted Tape Turbulator Using PCM Dispersed Mono/Hybrid Nanofluids, *Experimental Heat Transfer, 34* (2021), 5, pp. 421-442
[27] Bergles, A. E., *et al.*, Extended Performance Evaluation Criteria for Enhanced Heat Transfer Surfaces, *Letters in Heat and Mass Transferer, 1* (1974), Nov.-Dec., pp. 113-120
[28] Durán-Plazas, L.P., *et al.*, Mapping the Thermodynamic Performance of Turbulence Promoters, *Chemical Engineering Transactions, 94* (2022), Sept., pp. 67-72
[29] Picon-Nunez, M., *et al.*, Selection of Turbulent Promoters for Retrofit Applications Through Thermodynamic Performance Mapping, *Thermal Science and Engineering Progress, 42* (2023), 101876
[30] Zimparov, V. D., *et al.*, Benefits from the Use of Enhanced Heat Transfer Surfaces in Heat Exchanger Design, *Journal of Enhanced Heat Transfer, 23* (2016), 5, pp. 371-393
[31] Webb, R. L., Performance Evaluation Criteria for Use of Enhanced Heat Surfaces in Heat Exchanger Design, *International Journal of Heat and Mass Transfer, 24* (1981), 4, pp. 715-726
[32] Bejan, A., *Entropy Generation through Heat and Fluid Flow*, John Wiley & Sons, New York, USA, 1982, pp. 118-134
[33] Zimparov, V. D., *et al.*, Maximum Benefits from the Use of Enhanced Heat Transfer Surfaces, *International Communications in Heat and Mass Transfer, 134* (2022), 105992
[34] Zimparov, V. D., *et al.*, Performance Evaluation of Some Tube Inserts for Heat Transfer Enhancement: Twisted Tapes and Wire-Coils, *Journal of Gabrovo Technical University, 27* **(**2024), 8, pp. 39-46

Paper submitted: July 2, 2024
Paper revised: September 1, 2024
Paper accepted: September 4, 2024